www.sciencemag.org/cgi/content/full/324/5923/102/DC1

Supporting Online Material for

S-Nitrosylation of Drp1 Mediates β-Amyloid–Related Mitochondrial Fission and Neuronal Injury

Dong-Hyung Cho, Tomohiro Nakamura, Jianguo Fang, Piotr Cieplak, Adam Godzik, Zezong Gu, Stuart A. Lipton*

*To whom correspondence should be addressed. E-mail: slipton@burnham.org

Published 3 April 2009, *Science* **324**, 102 (2009)
DOI: 10.1126/science.1171091

This PDF file includes:

Supporting Online Materials

Supporting text

3D-deconvolution microscopy of NO-induced mitochondrial fission

A single image does not prove that mitochondrial fission has occurred. Hence, as previously reported *(1)*, we obtained QuickTime videos that unambiguously show the temporal changes in NO-induced mitochondrial fission using deconvolution microscopy. The images were then processed for 3D-reconstruction. Supplemental video 1a shows a low power movie of mitochondrial fragmentation in response to 200 μM SNOC with mitochondria labeled by mito-DsRed2 (http://www.nature.com/emboj/journal/v25/n16/extref/7601253s7.mov). Supplemental video 1b shows a higher power view of the same images, documenting mitochondrial fission in real time (http://www.nature.com/emboj/journal/v25/n16/extref/7601253s8.mov).

Materials and Methods

Plasmids and reagents

pMito-DsRed2 and pEGFPN1 were purchased from Clontech. pcDNA3-Drp1 and pcDNA3-Drp1 dominant negative (K38A) were kindly provided by Dr. A.M. van der Bliek (UCLA). Site directed mutagenesis was performed with the Quick change site-directed mutagenesis kit from Stratagene with pcDNA3-Drp1 as template. Each cysteine residue on Drp1 was substituted for an alanine residue. All mutants were confirmed by DNA sequencing. SNOC was prepared fresh following our prior protocol (*2*, *3*). The Aβ peptide 25-35 (Gly-Ser-Asn-Lys-Gly-Ala-Ile-Ile-Gly-Leu-Met) or control of the reverse sequence (ANASPEC, San Jose, CA) was dissolved in water and allowed to aggregate into soluble oligomers at RT for 24 h prior to treatment. Anti-Drp1 and anti-GFP antibodies were purchased from BD and Santa Cruz biotech.

Cell culture and transfection

HEK293 cells or HEK293 cells stably expressing nNOS (nNOS-HEK293) were cultured in DMEM with 10% FBS and 1% penicillin and streptomycin. N2a cells or N2a/APP695 cells stably expressing human APP695 (amyloid precursor protein, aa 1-695) were maintained in medium containing 50% DMEM, 50% Opti-MEM, and supplemented with 5% FBS. N2a/AP695 cells are known to secrete Aβ, which was collected as conditioned medium (*4*). Primary cortical neuronal cells were prepared as described previously (*1*, *3*). Cells were transfected using Lipofectamine 2000 (Invitrogen, Carlsbad, CA).

Biotin-switch assay

Analysis of SNO-Drp1 by the biotin-switch assay was performed as described (*3, 5*). Briefly, cells were lysed in with 1% Triton X-100 in HEN buffer (250 mM HEPES, 1 mM EDTA, 0.1 mM Neocuproine). Free thiols were blocked with methyl-methanethiosulfonate (MMTS). Cell extracts were precipitated with acetone and resuspended in HEN buffer with 1% SDS. Nitrosothiols were selectively reduced by ascorbate to reform the thiol group and subsequently biotinylated with 1 mM biotin-HPDP (Pierce, Rockford, IL). The biotinylated proteins were pulled down with streptavidin-agarose beads and analyzed by immuno blotting. Controls were performed lacking ascorbate to ensure specificity of the observed biotinylated bands.

Immunoblotting

Samples were extracted in sample buffer, separated by SDS-PAGE, and transferred to PVDF membrane. After blocking with skim milk in TBST, membranes were incubated with specific primary antibodies and HRP-conjugated secondary antibodies.

Fluorometric measurement of S-nitrosylated proteins with the DAN assay

SNO-Drp1 was measured with a modified 2,3-diaminonaphthalene (DAN) assay, as previously

described *(3, 6-9)*. Recombinant or purified Drp1 proteins were analyzed with this method. For purification of Drp1, HEK293 cells were transfected, exposed to SNOC, and then lysed. In brief, the lysates were immunoprecipitated for the transfected protein with agarose conjugated to anti-GFP antibody (Santa Cruz Biotech). After rinsing with phosphate-buffered saline, proteins were incubated with 200 μM HgCl2 and 200 μM DAN for half an hour in the dark. NO release from S-nitrosylated Drp1 was followed spectrofluorometrically, reflecting conversion of DAN to fluorescent 2,3-naphthyltriazole (NAT).

GTPase assay

GST-fused Drp1 proteins were expressed in bacteria and purified by using glutathione-sepharose 4B beads (Amersham Pharmacia Biotech, NJ). Purified proteins (20 μg) were exposed to old or fresh SNOC (200 μM) for 10 min at room temperature. GTPase activity was measured with a highly-sensitive GTPase assay kit by following enzymatic GTP hydrolysis activity in a plate reader at an absorbance of 635 nm, according to the manufacture's instructions (Innova Biosciences, UK).

Mitochondrial fragmentation and cell death assays

Cerebrocortical neuronal cells were transfected with pmito-DsRed2 and pDrp1. After 2 days, cells were exposed to SNOC (200 μM). Within 1 h, the mitochondria, which at baseline exhibited elongated tubular structures (fused condition) began to undergo fission into small, round dots (fragmented condition), as verified under deconvolution microscopy with 3D reconstruction (*1*, *10*). Volocity software (Improvision, Inc.) was employed for the 3D rendering of acquired z-stacks and for the quantification of mitochondrial length and number, as we have described previously (*1*). To monitor neuronal cell death, mixed cerebrocortical neurons and glia were grown on glass coverslips, transfected with pEGFP and pDrp1, and exposed to SNOC.

After 18 h, the cells were fixed in 4 % paraformaldehyde and then permeabilized with 1 % Triton X-100. After blocking, cells were incubated with anti-NeuN antibody (to identify neurons, Chemicon) and TRITC-conjugated secondary antibody. Nuclear morphology was evaluated by using Hoechst dye 3342 (Molecular Probe). Apoptotic neuronal death was determined by condensed nuclear morphology of EGFP/NeuN double-positive cells.

Homology modeling of human Drp1

For homology modeling, we chose the structure of bacterial dynamin-like protein (Bdlp) as a template (Protein Data Bank ID: 2J68-A). Although Bdlp has low sequence identity (12%) to human Drp1, the long sequence coverage (695 amino acids) and high FFAS score allowed us to reliably predict the structure of human Drp1 at the atomic level. For homology modeling and model building, we used the FFAS server (http://ffas.ljcrf.edu) and MODELLER program, as previously described (*11*, *12*). Subsequent molecular visualization and graphics handling were performed using PyMol. For superimposition of our atomic-resolution model of Drp1 onto a 3D cryo-EM image of the dimerized state, we used the low-resolution electron density map of the homologous ΔPRD dynamin molecule obtained by Zhang, Hinshaw, and colleagues (*13, 14*).

Quantification of dendritic spine density on cultured cortical neurons

CHO cells stably expressing human APP with the V717F mutation (7PA2 cells) secrete soluble monomers and low-*n* oligomers (dimers and trimers) of Aβ into the medium at a concentration similar to that found in human cerebrospinal fluid of patients with AD (*15*). In the present experiments, 7PA2 cells were grown to confluency and conditioned in Earle's balanced salt solution (plus 1.8 mM Ca2+) for 16 hr. The 7PA2-conditioned medium was cleared of cell debris by centrifugation (800 x *g* for 10 min) and concentrated 10-fold using VIVASPIN 15R (molecular weight cut-off of 2000), as described previously (*16*). Control conditioned medium

from wild-type (WT) CHO cells was prepared in the same manner. Concentrated media were aliquoted and stored at -80 °C until application to cultured cortical neurons. Cortical neuronal cultures were transfected at 14-16 days in vitro (DIV) with GFP and Drp1. Two days after transfection, neurons were exposed to the naturally-secreted Aβ conditioned medium for 5 days. For this incubation, we diluted the concentrated conditioned medium from 7PA2 or CHO cells with conditioned medium from cultured cortical neurons (1:10); 1 mM L-arginine was included in the medium to allow NO production by nNOS. Cultures were fixed in 4% paraformaldehyde (PF) for 10 min followed by permeabilization with 0.3% Triton X-100 in phosphate-buffered saline. Anti-NeuN (Chemicon) and anti-microtubule associated protein (MAP)-2 (Sigma) antibodies were used for immunocytochemistry to label neuronal cells. Images of GFPexpressing cells were acquired by deconvolution microscopy equipped with SlideBook 4.0 software (Intelligent Imaging Innovations, Inc., Santa Monica, CA). For GFP-expressing neurons ($n \geq 7$ for each condition), three distinct fields of secondary or tertiary dendrites were randomly selected and analyzed in a masked fashion.

Supplemental Figures and Legends

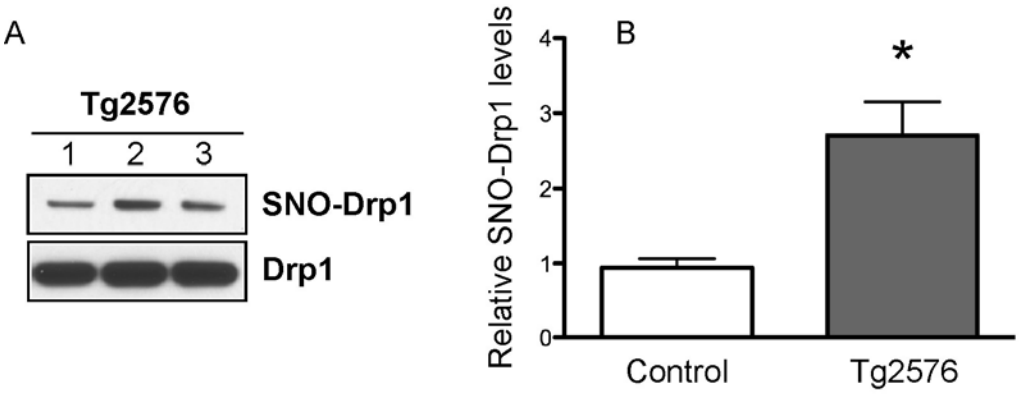

fig. S1. Increased SNO-Drp1 levels in mutant APP transgenic mice. **(A)** Brain tissue from three Tg2576 AD mice were subjected to the biotin-switch assay to detect SNO-Drp1 *in vivo*. Bottom panel represents total Drp1. (**B**) Relative levels of SNO-Drp1. Blots from the biotin-switch assay and immuno analyses were quantified by densitometry, and the relative ratio of SNO-Drp1 to total Drp1 calculated for Tg2576 AD and control mice. Values are mean + SEM, $n \geq 3$; $^{*}P < 0.002$ by *t*-test.

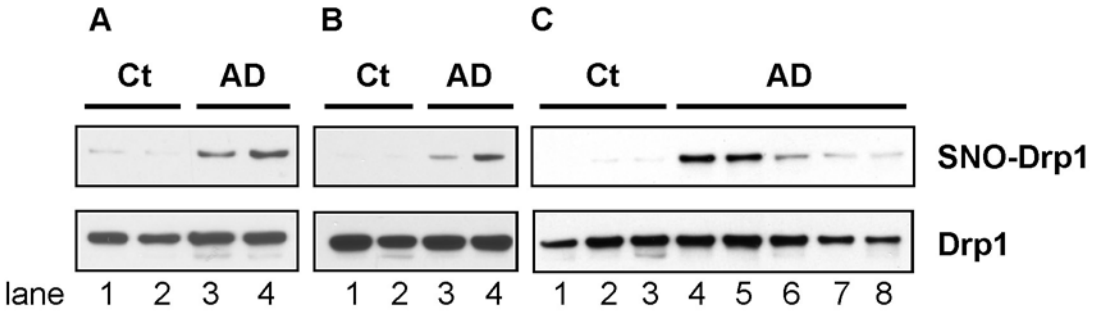

fig. S2. Additional human postmortem brain tissues from control (Ct) or AD patients were subjected to the biotin-switch assay to detect SNO-Drp1 in vivo. Separate blots are shown for different experiments (samples are described in Table S1). Bottom panel represents total Drp1.

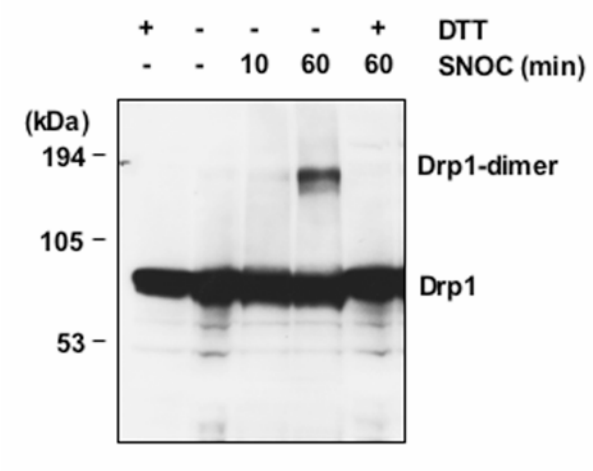

fig. S3. NO facilitates dimerization of endogenous Drp1 protein in cerebrocortical neurons. Cytosolic extracts from cortical neurons exposed to SNOC were immunoblotted with anti-Drp1 antibody and monitored temporally for dimerization of Drp1 by SDS-PAGE in the absence or presence of DTT.

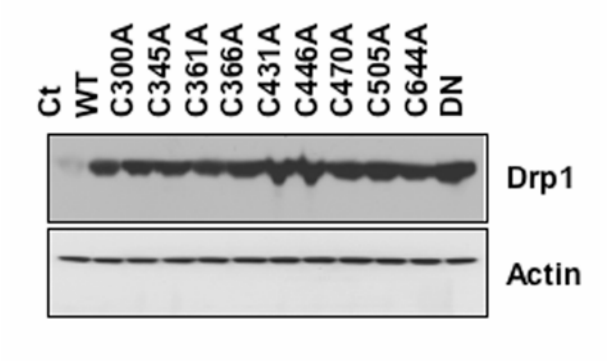

fig. S4. Expression of cysteine-mutant Drp1 proteins in HEK293 cells. HEK293 cells (control; Ct) were transfected with wild-type (WT), dominant negative (DN), or each cysteine-to-alanine (C to A) Drp1 mutant, and expression detected by immunoblotting with anti-Drp1 antibody. Actin was used as a loading control.

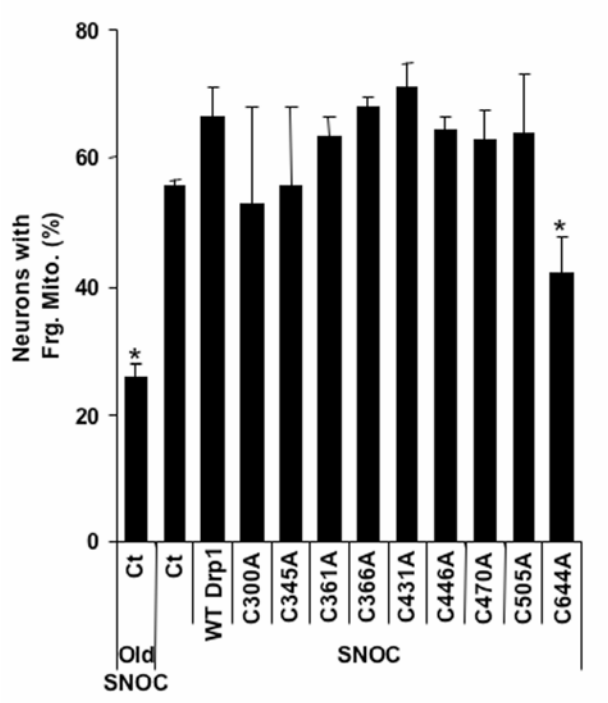

fig. S5. Effect on mitochondrial fragmentation of cysteine-mutant Drp1 proteins in cultured cortical neurons. Drp1 cysteine mutants, excluding Drp1(C644A), do not inhibit nitric oxide (NO)-induced mitochondrial fission. Cortical neurons, transfected with mito-DsRed2 alone (Ct) or mito-DsRed2 plus WT- or mutant-Drp1, were exposed to old or fresh SNOC (200 μM). After 1 h, a significant number of neurons exposed to the active NO donor exhibited fragmented mitochondria, except in the case of Drp1(C644A)-transfected neurons. Values are mean + SEM, $n \geq 3$; $^*P < 0.05$.

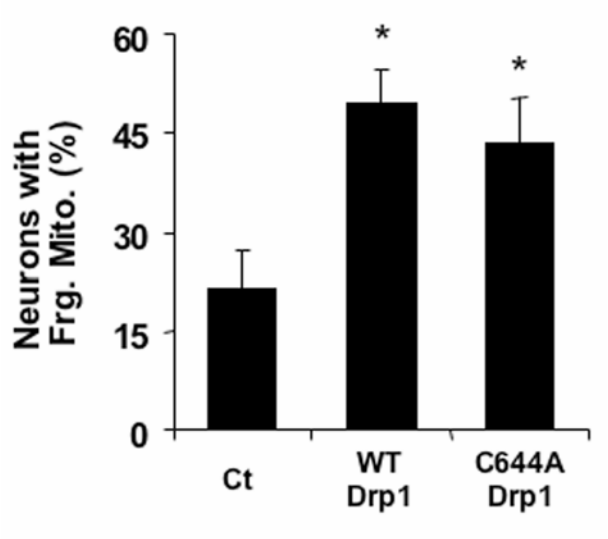

fig. S6. Drp1(C644A) does not act as a dominant negative for mitochondrial fission. Cortical neurons were transfected with mito-DsRed2 alone (Ct) or with mito-DsRed2 plus WT- or C644A mutant-Drp1 constructs. Overexpression of WT-Drp1 (2nd bar) increased mitochondrial fission compared to control containing endogenous Drp1 (1st bar), similar to results observed previously *(1)*. Expression of Drp1(C644A) also increased mitochondrial fission under these conditions (3rd bar), indicating that this construct did not act as a dominant negative for mitochondrial fission per se but did inhibit the component of NO-induced mitochondrial fission (as demonstrated in fig. S5). Values are mean + SEM, $n = 5$; $^*P < 0.01$.

Supplemental Table 1.

	Diagnosis	Brain region	PMI	Age	Gender	Lane # Fig. 2E	Bar # Fig. 2F	Lane # fig. S3A	Lane # fig. S3B	Lane # fig. S3C
Control 1	n/a	medial frontal cortex	9	102	Female	1	1	2		3
Control 2	Myocardial infarction	medial frontal cortex	2	71	Male	2	1	1	1	
Control 3	n/a	medial frontal cortex	24	69	Male	5	1			1
Control 4	Pneumonia	temporal cortex	n/a	87	Male	6	1			
Control 5	Bronchial pneumonia	frontal cortex	6	91	Male		1		2	
Control 6	Myocardial infarction	frontal cortex	8	63	Female		1			2
Patient 1	PD	medial frontal cortex	3	75	Female	7	7			
Patient 2	PD	temporal cortex	4	77	Female	8	7			
Patient 3	PD	temporal cortex	6	75	Female		7			
Patient 4	AD	medial frontal cortex	6	81	Female	3	6			
Patient 5	AD	medial frontal cortex	8	87	Male	4	6			
Patient 6	AD	frontal cortex	n/a	80	Female		6	3		
Patient 7	AD	frontal cortex	10	41	Female		6	4		
Patient 8	AD	frontal cortex	n/a	65	Male		6		3	
Patient 9	AD	frontal cortex	4	77	Male		6		4	
Patient 10	AD	frontal cortex	29	75	Male		6			4
Patient 11	AD	frontal cortex	11	78	Male		6			5
Patient 12	AD	frontal cortex	12	77	Male		6			6
Patient 13	AD	frontal cortex	n/a	76	Male		6			7
Patient 14	AD	frontal cortex	6	80	Male		6			8
Patient 15	AD	medial frontal cortex	7	86	Female		6			
Patient 16	AD	medial frontal cortex	8	88	Female		6			
Patient 17	AD	frontal cortex	19	68	Male		6			
Patient 18	AD	frontal cortex	14	86	Female		6			
Patient 19	AD	frontal cortex	3	77	Female		6			
Patient 20	AD	frontal cortex	n/a	83	Female		6			

Table S1. List of postmortem human brain samples used in this study. PMI: postmortem interval (in hours); AD: Alzheimer's disease; PD: Parkinson's disease with Lewy bodies.

Supplemental References

1. M. J. Barsoum *et al*., *EMBO J*. **25**, 3900 (2006).

2. S. Z. Lei *et al*., *Neuron* **8**, 1087 (1992).

3. T. Uehara *et al*., *Nature* **441**, 513 (2006).

4. W. J. Netzer *et al., Proc. Natl. Acad. Sci. USA* **100**, 12444 (2003).

5. S. R. Jaffrey *et al.*, *Nat. Cell Biol.* **3**, 193 (2001).

6. D. A. Wink et al., *Meth. Enzymol*. **301**, 201 (1999)

7. Z. Gu *et al*., *Science* **297**, 1186 (2002).

8. D. Yao *et al*., *Proc. Natl. Acad. Sci. USA* **101**, 10810 (2004).

9. N. Azad *et al*., *J. Biol. Chem*. **281**, 34124 (2006).

10. H. Yuan *et al.*, *Cell Death Differ* **14**, 462 (2007).

11. L. Jaroszewski, *et al*., *Nucl. Acids Res*. **33**, W284 (2005).

12. N. Eswar, *et al*., *Current Protocols in Bioinformatics*, (Wiley, New York, 2006), Supp. 15, Chap. 5.6.1.

13. P. Zhang, J. E. Hinshaw, *Nat. Cell Biol.* **3**, 922 (2001).

14. Y. J. Chen, P. Zhang, E. H. Egelman, J. E. Hinshaw, *Nat. Struct. Mol. Biol.* **11**, 574 (2004).

15. D. M. Walsh, *et al*., *Biochemistry* **39**, 10831 (2000).

16. G. M. Shanker *et al*., *J. Neurosci*. **27**, 2866 (2007).